COPY

(2)

DNA-TR-88-98-V3

AURORA UPGRADE

Volume III—Gradient B Drift Transport Risetime Sharpening

AD-A213 029

V. L. Bailey
Pulse Sciences, Inc.
600 McCormick Street
San Leandro, CA 94577

1 April 1988

Technical Report

CONTRACT No. DNA 001-85-C-0140

Approved for public release; distribution is unlimited.

THIS WORK WAS SPONSORED BY THE DEFENSE NUCLEAR AGENCY UNDER RDT&E RMC CODES X323085469 L B 00003 25904D AND B323085466 L B 00018 25904D.

Prepared for
Director
Defense Nuclear Agency
Washington, DC 20305-1000

DISTRIBUTION LIST UPDATE

This mailer is provided to enable DNA to maintain current distribution lists for reports. We would appreciate your providing the requested information.

- ☐ Add the individual listed to your distribution list.
- ☐ Delete the cited organization/individual.
- ☐ Change of address.

NAME: ______________________________

ORGANIZATION: ______________________________

OLD ADDRESS	CURRENT ADDRESS
______________	______________
______________	______________
______________	______________

TELEPHONE NUMBER: (   ) ______________________________

SUBJECT AREA(s) OF INTEREST:

______________ ______________

______________ ______________

______________ ______________

DNA OR OTHER GOVERNMENT CONTRACT NUMBER: ______________________________

CERTIFICATION OF NEED-TO-KNOW BY GOVERNMENT SPONSOR (if other than DNA):

SPONSORING ORGANIZATION: ______________________________

CONTRACTING OFFICER OR REPRESENTATIVE: ______________________________

SIGNATURE: ______________________________

CUT HERE AND RETURN

Director
Defense Nuclear Agency
ATTN: TITL
Washington, DC 20305-1000

Director
Defense Nuclear Agency
ATTN: TITL
Washington, DC 20305 1000

UNCLASSIFIED
SECURITY CLASSIFICATION OF THIS PAGE

REPORT DOCUMENTATION PAGE

1a REPORT SECURITY CLASSIFICATION UNCLASSIFIED	1b RESTRICTIVE MARKINGS
2a SECURITY CLASSIFICATION AUTHORITY N/A since Unclassified 2b DECLASSIFICATION/DOWNGRADING SCHEDULE N/A since Unclassified	3 DISTRIBUTION/AVAILABILITY OF REPORT Approved for public release; distribution is unlimited.
4 PERFORMING ORGANIZATION REPORT NUMBER(S) PSI-FR-219-03	5 MONITORING ORGANIZATION REPORT NUMBER(S) DNA-TR-88-98-V3
6a NAME OF PERFORMING ORGANIZATION Pulse Sciences, Inc. 6b OFFICE SYMBOL (if applicable)	7a NAME OF MONITORINNG ORGANIZATION Director Defense Nuclear Agency
6c ADDRESS (City, State, and ZIP Code) 600 McCormick Street San Leandro, CA 94577	7b ADDRESS (City, State, and ZIP Code) Washington, DC 20305-1000
8a NAME OF FUNDING/SPONSORING ORGANIZATION 8b OFFICE SYMBOL (if applicable) RAEV/Filios	9 PROCUREMENT INSTRUMENT IDENTIFICATION NUMBER DNA 001-85-C-0140
8c ADDRESS (City, State, and ZIP Code)	10 SOURCE OF FUNDING NUMBERS PROGRAM ELEMENT NO 62715H; PROJECT NO L; TASK NO B; WORK UNIT ACCESSION NO DH251447

11 TITLE (Include Security Classification)
AURORA UPGRADE
Volume III—Gradient B Drift Transport Risetime Sharpening

12 PERSONAL AUTHOR(S)
Bailey, V. L.

13a TYPE OF REPORT	13b TIME COVERED	14 DATE OF REPORT (Year, Month, Day)	15 PAGE COUNT
Technical	FROM 850201 TO 880331	880401	36

16 SUPPLEMENTARY NOTATION
This work was sponsored by the Defense Nuclear Agency under RDT&E RMC Codes X323085469 L B 00003 25904D and B323085466 L B 00018 25904D.

17 COSATI CODES			18 SUBJECT TERMS (Continue on reverse if necessary and identfy by block number)	
FIELD	GROUP	SUB-GROUP	Aurora Facility	SPEED
14	2		CASINO	Radiation Pulse
18	3			

19 ABSTRACT (Continue on reverse if necessary and identify by block number)

This report assesses the capability of gradient B drift transport to shorten both the risetime and duration of the Aurora radiation pulse. The theory of gradient B drift transport is reviewed, and experiments on both the CASINO simulator ~~at NSWC~~ and the SPEED accelerator ~~at SNLA~~ are summarized. Risetime shortening for Aurora is investigated, a possible experiment is defined, and a preliminary prediction of the Aurora radiation pulse shape is presented using gradient B drift transport. The report analyzes the effects which reduce radiation pulse spreading, and concludes that the gradient B drift transport is a promising backup/alternative to the Merkeltron for reducing the risetime of the Aurora radiation pulse.

20 DISTRIBUTION/AVAILABILITY OF ABSTRACT ☐ UNCLASSIFIED/UNLIMITED ☒ SAME AS REPORT ☐ DTIC USERS	21 ABSTRACT SECURITTY CLASSIFICATION UNCLASSIFIED	
22a NAME OF RESPONSIBLE INDIVIDUAL Bennie F. Maddox	22b TELEPHONE (Include Area Code) (202) 325-7042	22c OFFICE SYMBOL DNA/CSTI

DD FORM 1473, 84 MAR

83 APR edition may be used until exhausted
All other editions are obsolete

SECURITY CLASSIFICATION OF THIS PAGE
UNCLASSIFIED

TABLE OF CONTENTS

PREFACE

This volume is one of five volumes reporting the Aurora Upgrade Program conducted by Pulse Sciences, Inc. (PSI) under Contract No. DNA001-85-C-0140 from the Defense Nuclear Agency (DNA) for the Harry Diamond Laboratories (HDL). The five volumes are entitled:

Volume 1: Multipulse Modifications and Tests
Volume 2: High Power Microwave Environment
Volume 3: Gradient B Drift Transport Risetime Sharpening
Volume 4: Diverter Switch Pulse Shortening
Volume 5: Machine Monitoring and Control System

This work, which included PSI assisting HDL in reviewing and integrating associated Aurora Upgrade efforts being performed by other organizations, was performed over the period February 1985 through March 1988.

This volume examines risetime sharpening on Aurora using gradient B drift transport.

The DNA CTM was chronologically, Col. Jay Stobbs, Walt Jourdan, and Capt. Paul Filios. Dr. Jack Agee was the HDL technical and administrative authority. The program was managed by Philip Champney, and Vernon Bailey was the task leader.

CONVERSION TABLE

angstrom	1.000 000 X E -10	meters (m)
atmosphere (normal)	1.013 25 X E +2	kilo pascal (kPa)
bar	1.000 000 X E +2	kilo pascal (kPa)
barn	1.000 000 X E -28	meter^2 (m^2)
British thermal unit (thermochemical)	1.054 350 X E +3	joule (J)
calorie (thermochemical)	4.184 000	joule (J)
cal (thermochemical)/cm^2	4.184 000 X E -2	mega joule/m^2 (MJ/m^2)
curie	3.700 000 X E +1	*giga becquerel (GBq)
degree (angle)	1.745 329 X E -2	radian (rad)
degree Fahrenheit	$t_K = (t°f + 459.67)/1.8$	degree kelvin (K)
electron volt	1.602 19 X E -19	joule (J)
erg	1.000 000 X E -7	joule (J)
erg/second	1.000 000 X E -7	watt (W)
foot	3.048 000 X E -1	meter (m)
foot-pound-force	1.355 818	joule (J)
gallon (U.S. liquid)	3.785 412 X E -3	meter^3 (m^3)
inch	2.540 000 X E -2	meter (m)
jerk	1.000 000 X E +9	joule (J)
joule/kilogram (J/kg) (radiation dose absorbed)	1.000 000	Gray (Gy)
kilotons	4.183	terajoules
kip (1000 lbf)	4.448 222 X E +3	newton (N)
kip/inch^2 (ksi)	6.894 757 X E +3	kilo pascal (kPa)
ktap	1.000 000 X E +2	newton-second/m^2 (N-s/m^2)
micron	1.000 000 X E -6	meter (m)
mil	2.540 000 X E -5	meter (m)
mile (international)	1.609 344 X E +3	meter (m)
ounce	2.834 952 X E -2	kilogram (kg)
pound-force (lbs avoirdupois)	4.448 222	newton (N)
pound-force inch	1.129 848 X E -1	newton-meter (N·m)
pound-force/inch	1.751 268 X E +2	newton/meter (N/m)
pound-force/foot^2	4.788 026 X E -2	kilo pascal (kPa)
pound-force/inch^2 (psi)	6.894 757	kilo pascal (kPa)
pound-mass (lbm avoirdupois)	4.535 924 X E -1	kilogram (kg)
pound-mass-foot^2 (moment of inertia)	4.214 011 X E -2	kilogram-meter^2 (kg·m^2)
pound-mass/foot^3	1.601 846 X E +1	kilogram/meter^3 (kg/m^3)
rad (radiation dose absorbed)	1.000 000 X E -2	**Gray (Gy)
roentgen	2.579 760 X E -4	coulomb/kilogram (C/kg)
shake	1.000 000 X E -8	second (s)
slug	1.459 390 X E +1	kilogram (kg)
torr (mm Hg, 0° C)	1.333 22 X E -1	kilo pascal (kPa)

*The becquerel (Bq) is the SI unit of radioactivity; 1 Bq = 1 event/s.
**The Gray (Gy) is the SI unit of absorbed radiation.

LIST OF ILLUSTRATIONS

SECTION 1
INTRODUCTION

Experiments on both the CASINO simulator at the Naval Surface Weapons Center (Reference 1) and the SPEED accelerator at Sandia National Laboratories, Albuquerque (Reference 2), have shown that the risetime of the output radiation pulse can be shortened by extracting the beam from the diode and drifting the beam through a gradient B transport region. The converter in this case is at the end of the transport region. This report assesses the capability of gradient B drift transport to shorten both the risetime and duration of the radiation pulse on the Aurora generator.

The theory of gradient B drift transport is briefly reviewed in Section 2 and the experiments on CASINO and HYDRA are summarized in Section 3. Risetime shortening for Aurora is investigated in Section 4, and a possible experiment for Aurora is defined. A preliminary prediction of the radiation pulse shape for a gradient B drift transport on Aurora is also presented. Effects which reduce the risetime shortening are analyzed in Section 5. The summary and recommendations based on the investigation are contained in Section 6.

SECTION 2

GRADIENT B DRIFT TRANSPORT

A gradient B drift transport system consists of a current carrying wire along the axis of the transport region which is just beyond the diode. A sketch of the transport region showing the direction of the current in the axial wire and the coordinated system is shown in Figure 1. The background gas and gas pressure are chosen so that the beam is current and charge-neutralized almost instantly.

Since the beam is current and charge-neutralized there is no electric field acting on the beam electrons and the only magnetic field is the 1/r field from the wire current. The beam electrons undergo cycloidal motion with a net drift in the z-direction. The components of the guiding center drift velocity of the beam electrons are

$$
\begin{aligned}
v_D^z &= \frac{\gamma\, mc^2}{2\, e\, B_\theta\, r} \left[\left(1 - 1/\gamma^2\right) + \frac{v_\theta{}^2}{c^2}\right] \\
v_D^\theta &= v_\theta \qquad\qquad (1) \\
v_D^r &= 0
\end{aligned}
$$

where m is the rest mass of the electron, c is the speed of light, e is the electronic charge, γ is the relativistic factor, B_θ is the magnetic field of the wire current at the radius r, and v_θ is the azimuthal velocity of the beam electrons. If the beam is azimuthally symmetric and is generated in a diode without an external magnetic field, the $v_\theta{}^2/c^2$ term is small and the drift velocity is only in the z-direction

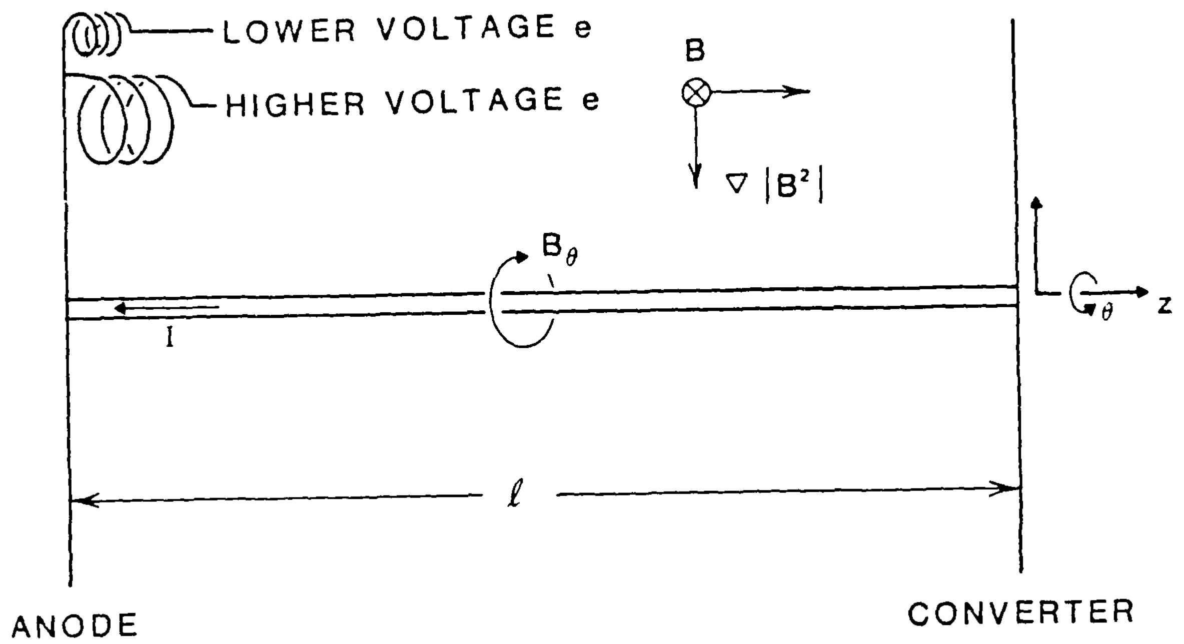

Figure 1. Sketch of the drift region for gradient B beam transport showing the coordinate system and direction of current in the axial wire.

$$v_D^z = \frac{mc^2 \gamma}{2\ e\ B_\theta\ r} (1 - 1/\gamma^2) \ . \tag{2}$$

The drift velocity is proportional to $\beta^2\gamma$ and is independent of injection radius since B_θ r depends only on the current in the wire.

During the rising portion of the diode voltage pulse, lower energy beam electrons which are injected into the transport region earlier in time, drift more slowly than the higher energy electrons which are injected later in time. The higher energy electrons overtake the lower energy electrons, resulting in longitudinal current bunching at the converter. This can decrease the risetime of the radiation pulse and increase the maximum dose rate. The amount of current bunching depends on the current in the wire, the drifted distance, and the shape of the diode voltage pulse (both γ-dot and γ).

Voltage pulses which rise like t^n with $n < 1$ tend to produce less current enhancement than voltage pulses which rise like t^n with $n > 1$. The expression for the current enhancement factor as a function of drifted distance, wire current, diode voltage and rate of change of diode voltage is given in Reference 3.

During the falling portion of the voltage pulse, debunching occurs and the dose rate drops rapidly.

The potential advantages of using gradient B drift transport on Aurora are:

(1) After gradient B transport, the risetime of the radiation pulse can be much less than the risetime when the converter is placed at the anode plane.

(2) The maximum radiated power can be increased.

(3) The beam can follow a curved wire path. In principle, the beam can be bent through rather large angles by this technique.

(4) The risetime of the radiation pulse and the maximum dose rate can be adjusted by changing the wire current.

(5) There is no (or minimum) magnetic field in the radiation test volume.

(6) The technique can be used with the existing Aurora facility with only a minimum of additional hardware.

The disadvantages are that radiation power is decreased during the falling portion of the voltage pulse and the gradient B system adds complexity to the experiment. Another potential disadvantage is that the gradient B drift transport may increase the average angle of incidence of the electrons on the converter. This effect is discussed further in Section 5.

SECTION 3
EXPERIMENTAL RESULTS

Gradient B drift transport experiments have been carried out on the CASINO accelerator at the Naval Surface Weapons Center (NSWC) and the HYDRA accelerator at Sandia National Laboratories, Albuquerque (SNLA).

In the CASINO experiments (Reference 1) transport efficiencies, based on radiation production in the converter, of 80-90% were regularly observed for a transport distance of 1.85 meters with currents in the wire of 100-160 kA. The transport efficiency was independent of pressure for pressures of 1-10 torr in the transport region but decreased rapidly for pressures above 10 torr. Radiation risetime compression of up to a factor of two was inferred by comparing the risetime of the radiation from electrons striking material at the entrance to the transport region to the risetime of radiation from the downstream converter.

The drift velocity inferred from the difference in time between the initiation of the two radiation signals (from entrance material and downstream converter) was within 17% of that predicted by theory. The theoretically predicted dose rate increases were not observed experimentally. Subsequent analysis (Reference 1) of the experiments showed that the three-pronged (crow's foot) current feed technique produced a non-azimuthally symmetric B_z field in the diode which cancelled the beam bunching predicted by theory.

The gradient B experiments on the HYDRA accelerator (Reference 2) were carried out at approximately the same time as the CASINO experiments. The drift region was 89 cm long and the wire currents were between 5 and 75 kA. The experimentally measured electron drift velocity was in good agreement with the theoretically predicted value over the entire range of wire currents used. Efficient beam transport was inferred from measurements of X-ray production at the target.

In subsequent experiments on SPEED at SNLA by J.R. Lee (Reference 4), the 25 ns standard diode current risetime on SPEED was reduced to a 3 ns radiation pulse risetime (0-peak) after gradient B transport. Because of difficulties with the diode transport region interface, only 50% of the beam was injected into the transport region. An improved design for the interface region is expected to significantly increase the fraction of the beam injected into the transport region without significantly increasing the radiation risetime.

SECTION 4
RISETIME SHARPENING FOR AURORA

Assuming that the Aurora beam which we are attempting to bunch is azimuthally symmetric and is generated in a diode without an external magnetic field, the drift velocity is then only in the z-direction (along the wire axis) and is given in terms of the wire current, I_w, by

$$v_D^Z = \frac{\pi \, mc^2 \, \gamma}{e \, \mu_o \, I_w} \, (1 - 1/\gamma^2) \quad . \tag{3}$$

Since the drift velocity is independent of the drifted distance, the important quantity in designing a risetime sharpening experiment is the product of the drifted distance and the wire current which is given by

$$\Delta Z \, I_w = \frac{\pi \, mc^2}{e \, \mu_o} \, \gamma \, (1 - 1/\gamma^2) \, \Delta t \, . \tag{4}$$

where ΔZ is the distance drifted by an electron in a time Δt. If the units are changed to ΔZ in meters, I_w in 100 kA, and Δt in nanoseconds, the product $\Delta Z \, I_w$ (m - 100 kA) becomes

$$\Delta Z \, I(\text{m} - 100 \text{ kA}) = 0.0128 \, \gamma \, (1 - 1/\gamma^2) \, \Delta t \, (\text{ns}) \quad . \tag{5}$$

The most direct method for choosing the desired transport distance, ΔZ, and wire current, I_w, is to construct a $\Delta Z \, I_w$ versus t plot for electrons injected into the transport region at various times within the pulse. These types of plots are similar in purpose to the standard x-t plots used in shock physics.

The $\Delta Z\ I_w$ - t plot for a gradient B experiment on Aurora is shown in Figure 2. The diode voltage waveform which was used to construct the $\Delta Z\ I_w$ - t plot is based on Aurora shot number 4833 and is shown in Figure 3. The diode voltage was obtained by using the measured diode current and assuming a constant impedance diode. The diode voltage was then scaled to a 10 MV peak voltage.

The $\Delta Z\ I_w$ - t plot provides the following information. For $2 \leq \Delta Z\ I_w \leq 9.3$ (dimensions are meters times hundreds of kiloamperes), electrons injected at t = 50 ns (4.1 MV) are the first to arrive at the converter (the pulse was divided into 12.5 ns intervals). For $\Delta Z\ I_w = 7$, the electrons injected from t = 50 ns (4.1 MV) to t = 112.5 ns (9.1 MV), arrive at the converter within 30 ns. Folded on top of these electrons are electrons which were generated between t = 37.5 ns (2.2 MV) and t = 50 ns (4.1 MV). Electrons injected between t = 0 and t = 37.5 ns arrive later.

For the possible experiment on Aurora we choose a $\Delta Z\ I_w$ product of 12.5 (m - 100 kA). For this case electrons injected at t = 87.5 ns (7.5 MV) are the first to arrive. Electrons injected between t = 87.5 ns and t = 112.5 ns (9.1 MV) arrive within the next 15 ns. Folded on top of these electrons are electrons which were injected between t = 50 ns (4.1 MV) and t = 87.5 ns (7.5 MV).

The amount of risetime compression and bunching which occurs depends on the shape of the injected voltage pulse and the product of the gradient B transport distance and the wire current. Shorter transport distances with larger wire currents are equivalent to longer transport distances with less wire current. For the potential Aurora experiment we choose a wire current of 357 kA and a transport distance of 3.5 meters.

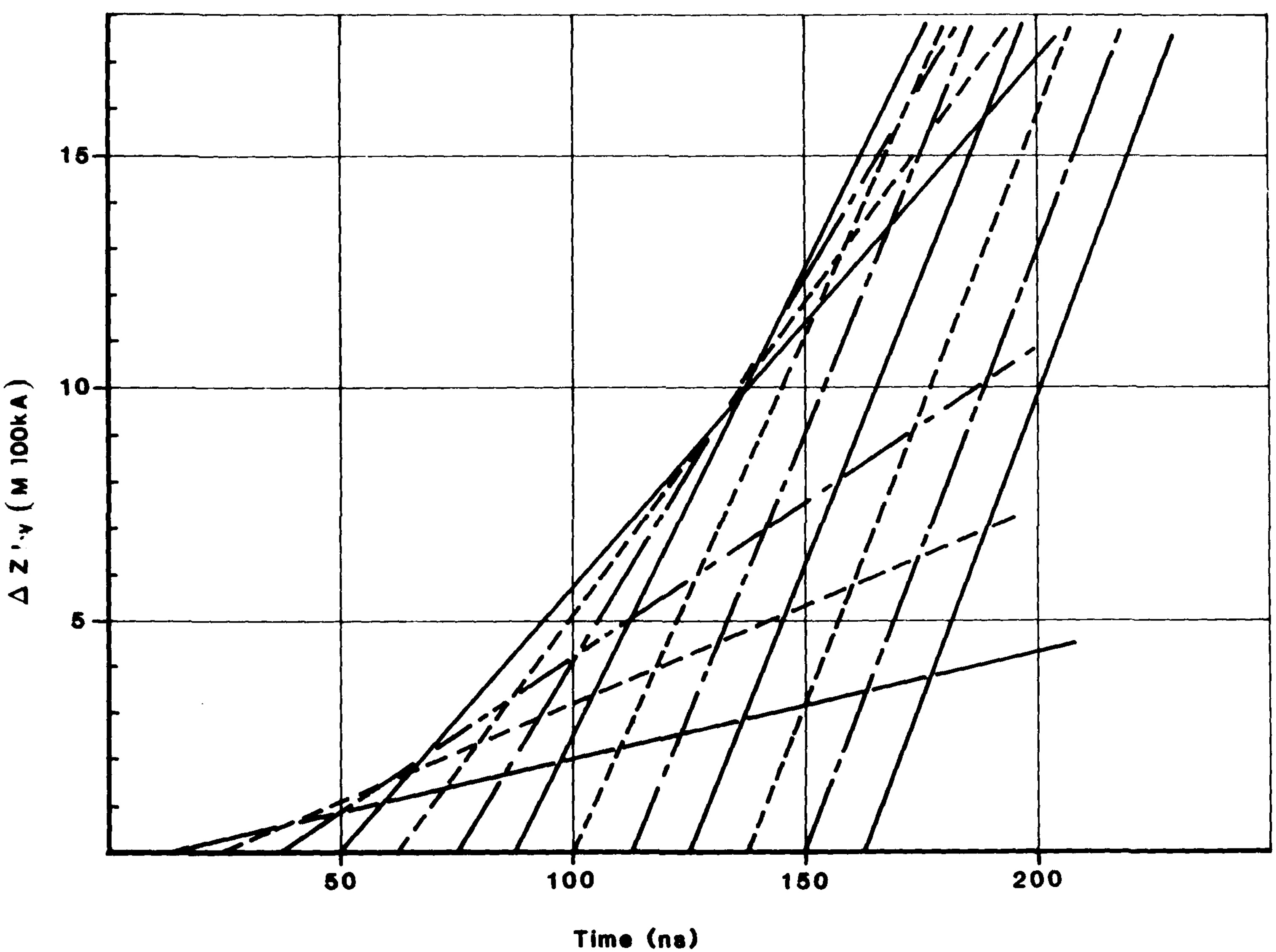

Figure 2. $\Delta Z\ I_W$ - t plot for electrons in a gradient B drift transport experiment on AURORA. The diode voltage is scaled from AURORA shot number 4833.

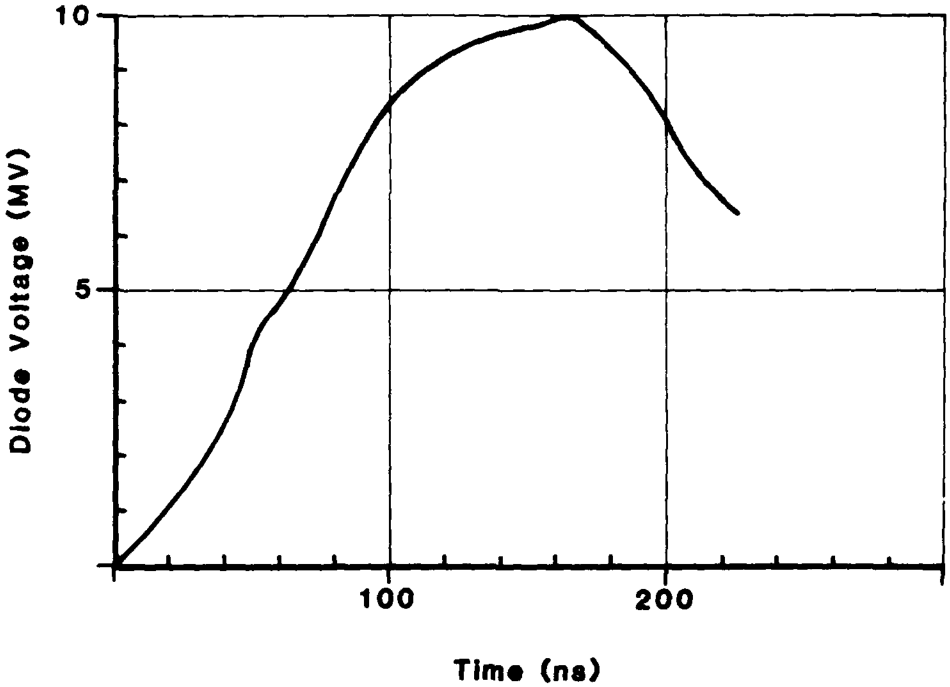

Figure 3. AURORA diode voltage used to construct $\Delta Z\ I_w$ - t plot. Diode voltage scaled from AURORA shot number 4833.

For electrons with an incident velocity vector which is perpendicular to the plane of the converter, the dose rate in air is given by $V^{2.65}$ I for voltages from 1-10 MV. This scaling is based on electron/photon Monte Carlo transport runs (Reference 5) and the empirical formula of Martin (References 6 and 7). Assuming that the diode impedance is constant, the dose rate becomes proportional to $V^{3.65}$. The Aurora beam has a spectrum of angles of incidence which reduce the voltage dependence of the dose rate to approximately V^3 for a converter at the anode.

If the effective angular spectrum of the incident electrons is unchanged after gradient B transport, the dose rate in air should be proportional to $V^3\eta$. The factor η is the current enhancement due to gradient B beam bunching.

Applying the $V^3\eta$ scaling to the potential experiment on Aurora with $\Delta Z\ I_w = 12.5$ (m - 100 kA) and normalizing to the dose rate at the 10 MV peak voltage without any current enhancement, the predicted normalized dose rate for the gradient B transport experiment is shown in Figure 4. For comparison, the predicted normalized dose rate for a converter placed at the anode plane is also shown in Figure 4. The predicted 85 ns 10-90% risetime of the radiation pulse for a converter placed at the anode plane of Aurora, is reduced to 5 ns for a converter placed at the end of the $\Delta Z\ I_w = 12.5$ gradient B transport region. Since there are several effects which have been neglected in constructing Figure 4 and which tend to increase the risetime of the radiation pulse, a more realistic estimate of the risetime of the radiation pulse aftr gradient B transport is 10-15 ns. Several of these effects are analyzed in Section 5.

In order to evaluate a potential gradient B transport experiment on Aurora, assumptions concerning the experimental

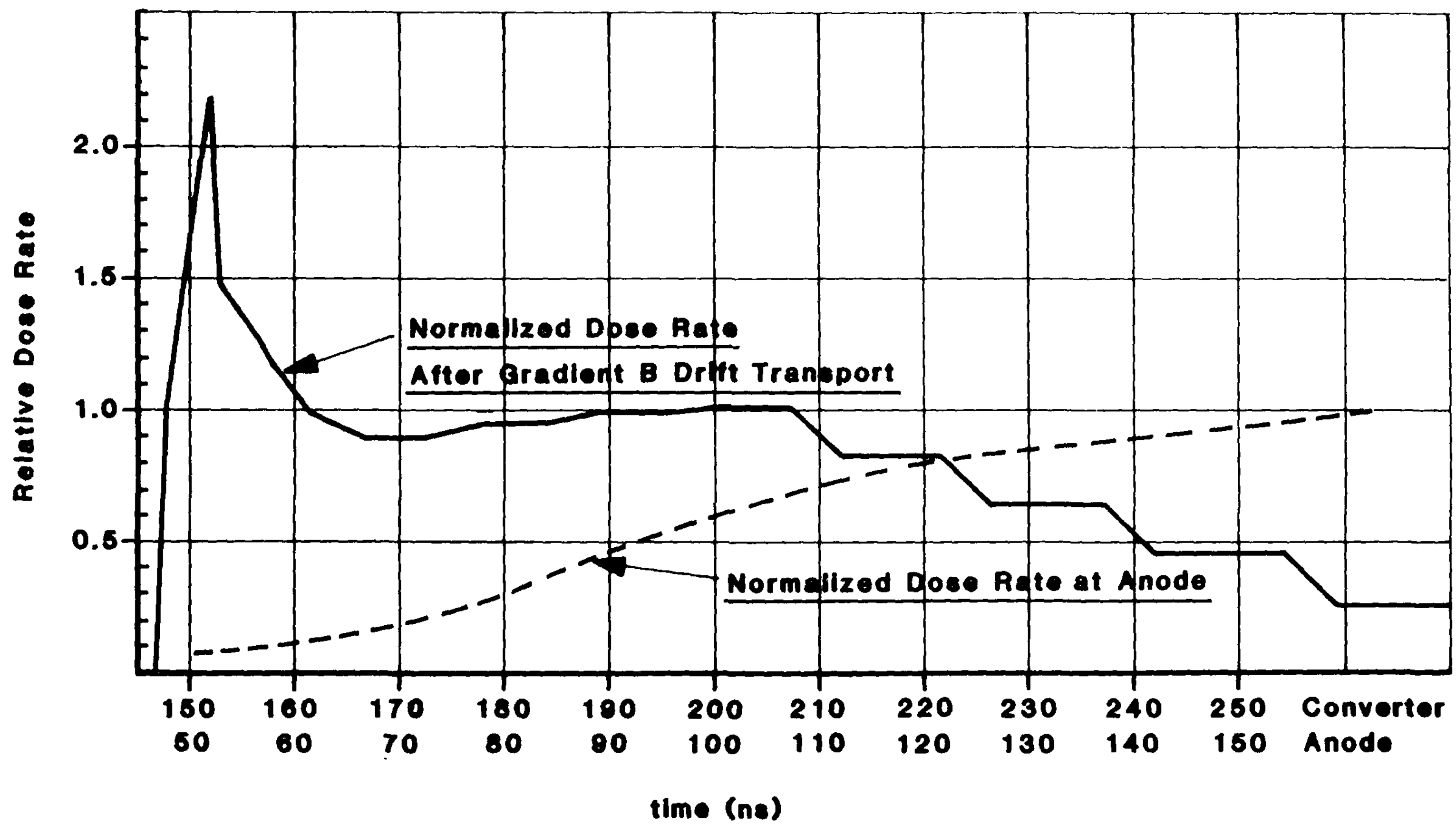

Figure 4. Predicted normalized dose rate for AURORA beam after gradient B drift transport of 3.5 m with a wire current of 357 kA. Assumes angular spectrum unchanged by gradient B drift transport. Normalized dose rate at anode included for comparison.

equipment were made. While these assumptions are realistic, no attempt was made to optimize the experiment.

Assuming the on-axis wire, or rod in this case, has a radius of 2.54 cm and an effective return current radius of 90 cm, the inductance per unit length for the transport region is

$$\frac{L}{\ell} = 5.96 \times 10^{-7} \text{ H/m} \quad . \tag{6}$$

The inductance of the 3.5 meter transport distance for the potential experiment is $L = 2.1 \times 10^{-6}$ H. The magnetic field energy required for the potential experiment is 134 kJ. We estimate that a 200-250 kJ capacitor bank should be adequate for the experiment.

The capacitor bank could be composed of eight 500 μF capacitors charged to 10 kV. Neglecting the inductance and resistance of the bank and feed cables, the current risetime of the 4 mF bank into the 2.1 μH inductance of the transport region is 144 μs with a peak current of 436 kA available at 10 kV.

One of the potential problem areas is the current carrying foil at the entrance to the transport region. As a solution we envision a layered foil composed of the standard (Reference 8) 16 mil thick titanium transmission window backed with a 10 mil thick aluminum foil.

The titanium foil will support the pressure differential between the transport region and the diode. For the gradient B transport experiment the foil must also support the magnetic field pressure in the transport region. The total magnetic field force on the entrance foil is 37978 nt (8537 lbf) which corresponds to an average pressure of 7 psi. Unfortunately most of the force is concentrated near the center. Attaching the titanium transmission foil to the axial current carrying rod, which can be held fixed, will provide support to the center of the foil.

The purpose of the aluminum is to carry the 357 kA current. For the risetime of 144 μs and an axial rod radius of 2.54 cm, the maximum specific action in the aluminum is 4550 (amp^2 sec/mm^4) and 18 (amp^2 sec/mm^4) in the titanium which, due to resistive division, carries approximately 10% of the current. The foil should be in no danger of melting since the specific action is 25238 (amp^2 sec/mm^4) for aluminum at begin melt, and 3034 (amp^2 sec/mm^4) for titanium at begin melt.

The RMS scattering angle acquired by the beam electrons as they pass through the foil is $\approx$ 10-12 degrees. Since the maximum current density for the Aurora beam occurs at r > 2.54 cm, the axial current carrying rod will intercept less than 7% of the beam. This estimate includes the finite gyroradius effects of electrons injected at r > 2.54 cm.

Gradient B drift transport of the Aurora beam offers the potential for reducing the risetime of the output radiation pulse to less than 15 ns while increasing the peak radiated power by as much as a factor of two. A short expansion or inverse gradient B region may be needed to give an outward radial component to the electron velocity vector prior to injection into the gradient B transport region.

SECTION 5

EFFECTS WHICH PRODUCE RADIATION PULSE SPREADING

There are several effects which tend to increase the rise-time and/or decrease the beam bunching. Among these are:

(1) The drift approximations used to obtain the expression for the drift velocity are only valid in the limit of large on-axis currents. For smaller currents the drift velocity expression contains additional terms which tend to reduce the beam bunching from that predicted by the simple theory.

(2) The beam electrons are injected into the transport region with a spread in injection angles. This injection angle spread leads to debunching of the beam electrons at the downstream converter.

(3) The beam electrons undergo cycloidal motion as they propagate. Thus the angle of the electron velocity vector with respect to the Z-axis changes as the electron propagates. Electrons which are injected parallel to the axis may have a larger angle with respect to the axis when they intercept the converter. This effect is important because the dose in the radiation volume of interest depends on the angle of incidence of the electrons at the converter.

(4) The scattering of the beam electrons as they pass through the entrance foil changes the angular spectrum of the electron.

(5) Not all the injected electrons propagate. Some of the electrons intercept the axial wire, and some electrons which are injected with too large an angle with respect to the Z-axis, re-enter the diode.

(6) Because of non-complete current neutralization of the beam, the azimuthal magnetic field is not proportional to (1/R). The effect causes the drift velocity to be a function of radius.

(7) The small, but finite axial electric field required to maintain the plasma return currents can also affect the beam bunching.

Before examining these effects in more detail the equations of motion for a electron in the azimuthal magnetic field are considered. The equations of motion are given by

$$\ddot{R} = - \frac{e\,\dot{Z}\,B_o}{\gamma m}\left(\frac{R_o}{R}\right)$$

$$\ddot{Z} = \frac{e\,B_o\,R_o}{\gamma m}\left(\frac{\dot{R}}{R}\right) \qquad (7)$$

where $B_\theta = B_o\,(R_o/R)$, R_o is the injection radius, and the dot represents a time derivative. The equations of motion along with the initial conditions at the injection plane determine the electron trajectory in the transport region. The non-dimensional radius, $\breve{R}$, axial propagation distance, $\breve{Z}$, and time, $\breve{t}$, are defined as

$$\begin{aligned} \breve{R} &= R/R_o \\ \breve{Z} &= Z/R_o \\ \breve{t} &= t/(\gamma\, m/e\, B_o) \end{aligned} \qquad (8)$$

where R_o is the injection radius and B_o is the magnetic field at the injection radius. Substituting the non-dimensional variables into the equations of motion gives

$$\begin{aligned} \ddot{\breve{R}} &= -\,\dot{\breve{Z}}/\breve{R} \\ \ddot{\breve{Z}} &= \dot{\breve{R}}/\breve{R} \end{aligned} \qquad (9)$$

along with the initial conditions

$$\dot{\tilde{R}}(o) = -0.5\ (I_A/I_w)\ \sin \alpha_o$$

$$\dot{\tilde{Z}}(o) = 0.5\ (I_A/I_w)\ \cos \alpha_o \tag{10}$$

where the angle α is defined as $\alpha = \tan^{-1}(-R/Z)$ and α is equal to α_o at the injection plane. The Alfven current I_A is defined as $I_A = 1700\ \beta\gamma$.

The primary variables which determine the electron trajectory are the ratio of the Alfven current to the wire current and the initial injection angle α_o. The primary variable list is further reduced when we realize that the $\alpha_o \neq 0$ trajectory can easily be scaled from the $\alpha_o = 0$ trajectory.

The previous expression for the drift velocity becomes

$$V_D = 0.25\ \beta\ c\ (I_A/I_w) \tag{11}$$

in terms of the ratio I_A/I_w. This expression is only strictly valid in the limit of $I_w >> I_A$. The more general expression for the drift velocity which applies for all values of I_A/I_w is given by

$$V_D = 0.25\ \beta\ c\ (I_A/I_w)\ g\ (I_A/I_w) \tag{12}$$

where $g\ (I_A/I_w)$ is a slowly varying function of I_A/I_w and is shown in Figure 5.

The maximum value of I_A/I_w for the gradient B risetime sharpening experiment on Aurora is $I_A/I_w = 0.98$. The 3% dispersion in the drift velocity for this value of I_A/I_w has only a minor effect (< 5%) on the risetime sharpening predictions in Section 4. The effect becomes even less when we realize that

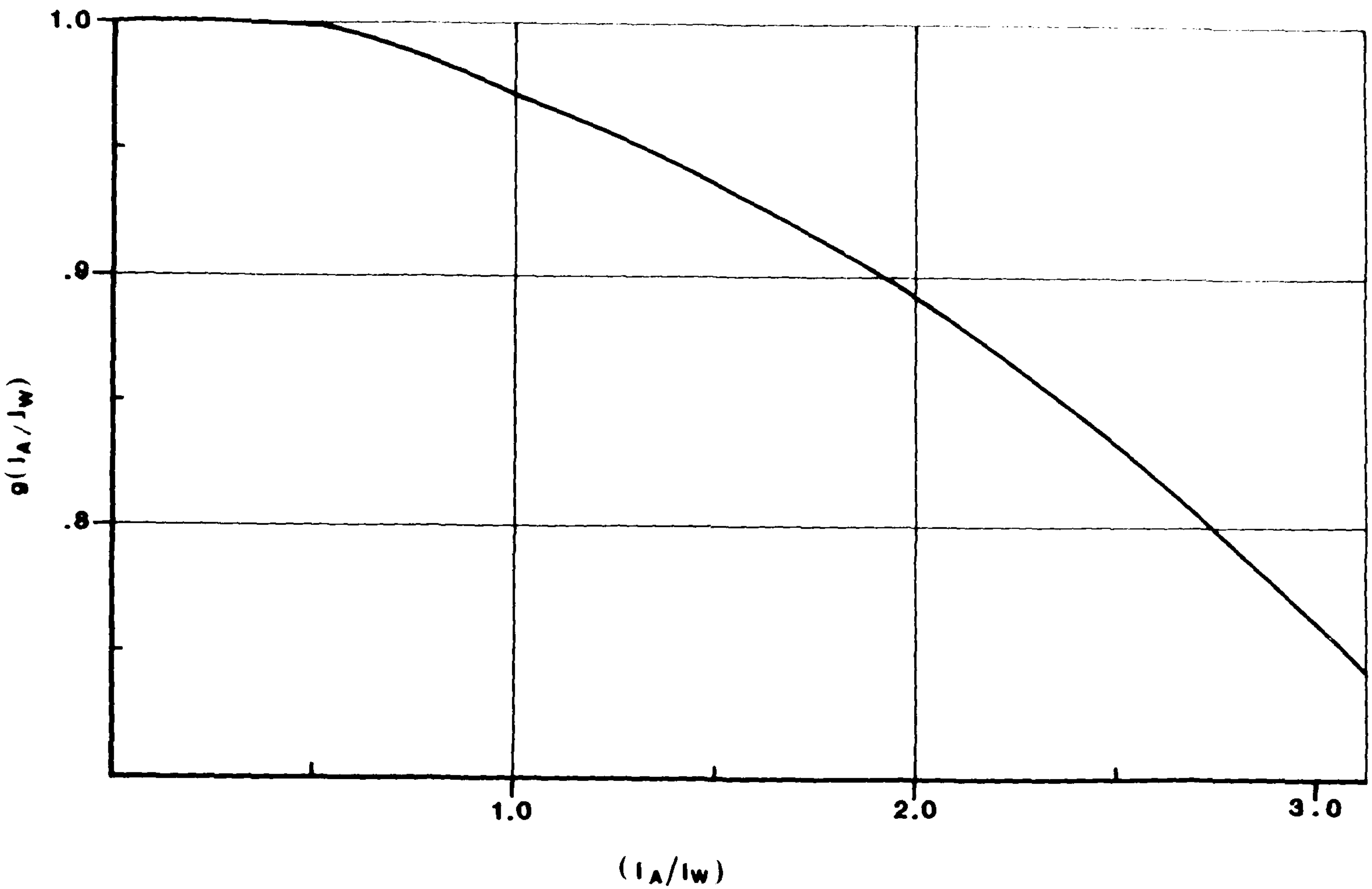

Figure 5. Gradient B drift velocity correction as a function of I_A/I_W; $V_D = \beta c/4\ (I_A/I_W)\ g(I_A/I_W)$.

most of the beam bunching occurs around 8 MV, and at 8 MV g = 0.988 (≈ 1.2% dispersion in velocity).

Some of the injected electrons may intercept the axial current carrying wire or rod. For the potential Aurora experiment, the axial rod will intercept < 7% of the injected current

The gradient B transport region has an acceptance angle for injected electrons which is a function of I_A/I_W. Electrons which are injected with an angle larger than the acceptance angle, spiral back into the diode and do not propagate. The acceptance angle for the injected electrons is given in Reference 9. We note in passing that the diode for the potential Aurora experiment can be redesigned so that most of the injected electrons will be within the acceptance angle. For a given wire current, the acceptance angle increases as the kinetic energy of the injected electrons increase. This effect can also be used to decrease the risetime of the radiation pulse.

Electrons injected at the same time and at the same radial position with different initial injection angles will arrive at the converter at different times. Figure 6 shows the effect of different initial injection angles on two electron trajectories for $I_A/I_W = 2$. The two injection angles, $\alpha_o = 30^o$ and $\alpha_o = -90^o$ represent the upper and lower bonds on the acceptance angle. The spread in arrival times of the two electrons depends on the position of the converter but in no case will it be larger than the time between the two limit lines shown in Figure 6.

Numerical solutions of the equations of motion demonstrate that the maximum spread in arrival times due to injection angle spread can be written as

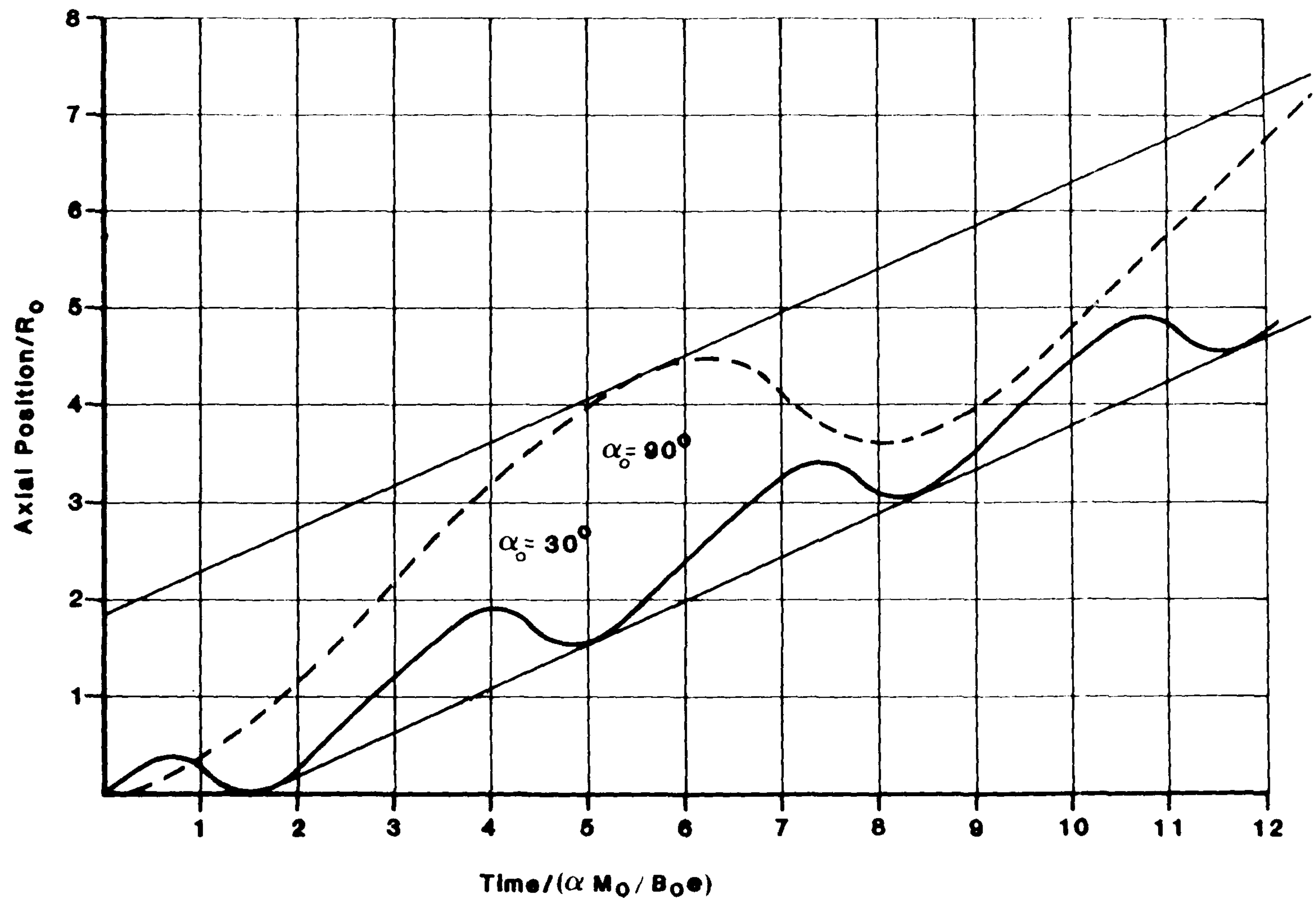

Figure 6. Effect of injection angle spread on electron trajectories for $I_A/I_w = 2.0$. Initial injection angles are $\alpha_o = 30^\circ$ and $\alpha_o = -90^\circ$.

$$\Delta t_R = \frac{R_o}{\beta c} f \; (I_A/I_w) \qquad (13)$$

where f is a slowly varying function of (I_A/I_w). Figure 7 shows the variation of (f) as a function of I_A/I_w and includes a curve fit, to the five numerical data points.

Injection angle spread limits the amount of beam bunching which can be obtained. Tne injection angle spread can either occur in the diode or can be due to the scattering of beam electrons as they pass through the entrance foil. Of all of the effects considered which produce pulse spreading on Aurora, injection angle spread has the largest effect on risetime compression. For this reason, the risetime sharpening prediction shown in Figure 4 for the potential Aurora gradient B experiment includes the maximum amount of injection angle spread.

The angle of the beam electron velocity vector with respect to the Z-axis changes as the electron propagates. Electrons which are injected parallel to the axis may have a larger angle with respect to the axis when they intercept the converter.

As an example, consider three electrons injected at a radius R_o into a gradient B transport region with $I_A/I_w = 2.0$. The electrons are injected with three different initial values of α_o [$\alpha = \tan^{-1} (- v_R/v_Z)$] ranging from 0^o to 30^o. Table 1 summarizes the results obtained by solving the equations of motion. After propagating a distance of 1.04 R_o, the electron injected with $\alpha_o = 0$ has $\alpha_1 = 0$, while the electrons injected with $\alpha_o = 15^o$ and 30^o have angles of $\alpha_2 = 12.3^o$ and $\alpha_3 = 19^o$ respectively. The spread in angles continues to decrease until the propagation distance reaches 3.11 R_o.

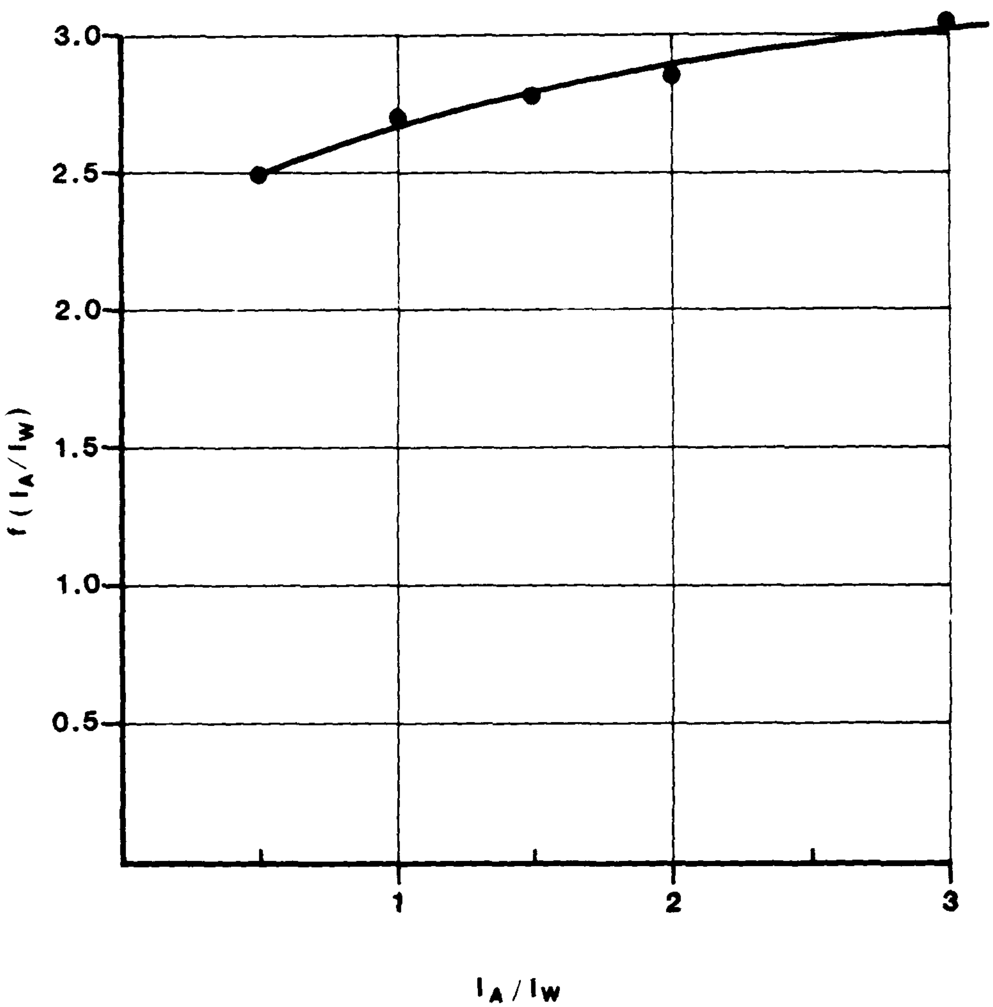

Figure 7. Maximum spread in arrival time at the converter due to injection angle spread. The maximum spread in arrival times is given by $\Delta t_r = (R_o/\beta_c)\ f(I_A/I_W)$.

Table 1. Angle with respect to Z-axis as a function of propagation distance for three different injection angles and $I_A/I_W = 2.0$.

Z/R_o	α_1 (degrees)	α_2 (degrees)	α_3 (degrees)
0	0	15.0	30
1.04	0	12.3	19
2.08	0	9.7	8
3.11	0	7.1	-3
4.15	0	4.5	-14
5.19	0	1.9	-25

The radiation dose in the volume of interest depends on the angle of incidence of the electrons at the converter. After gradient B transport the electron beam may be more or less efficient in producing radiation in the volume of interest. The angular spectrum and therefore the efficiency depend on the injection radius, angular spectrum at injection, I_A/I_W, and the transport distance.

Numerical particle orbit simulations, which are beyond the scope of the present effort, are required to resolve the efficiency issue. The prediction for the risetime shortening on Aurora shown in Figure 4 assumes that the angular spectrum is unchanged by gradient B transport.

The effects of incomplete current neutralization and the axial electric field required to maintain the plasma return current are expected to be small for the potential gradient B experiment on Aurora. Lee of SNLA (Reference 10) has evaluated both effects in detail.

SECTION 6
SUMMARY AND RECOMMENDATIONS

Gradient B drift transport of the Aurora beam offers the potential for reducing the risetime of the output radiation pulse to less than 15 ns. The theoretical analysis, which led to this conclusion, used a diode voltage waveform based on Aurora shot number 4833. The gradient B transport distance was 3.5 meters with an on-axis wire current of 357 kA. The output radiation after gradient B transport was assumed to be proportional to V^3 times the current enhancement factor η.

The risetime sharpening estimates included the effect of injection angle spread but assumed that the effective angular (angle of incidence) spectrum remained unchanged after gradient B transport. Numerical simulations with existing (PSI and SNLA) gradient B transport codes should be done to resolve this issue prior to experiments on Aurora.

A preliminary conceptual design of a potential gradient B transport experiment on Aurora was also carried out. No fundamental physics or engineering problems arose as a result of conceptual engineering design of the overall experiment. The present vacuum tank for the Merkeltron experiment could be used for a gradient B experiment. Th on-axis current conductor for the experiment would be a 2 inch OD cylindrical tube which could be designed to help support the entrance foil. As presently envisioned, the entrance foil would consist of a 16 mil titanium foil to support the pressure gradient across the foil and an attached 10 mil aluminum foil to carry the wire current.

The wire current for the experiment could be provided by a 200 kJ (4 mF, 10 kV) capacitor bank. Unfortunately while the bank energy for the gradient B experiment is similar to the energy of the B_z diode bank, the current required for the 5-15 ns risetime gradient B experiment is much larger than the maximum current available from the B_z diode bank. Useful gradient B scaling experiments could, however, be done with the B_z diode bank, but the risetime of the radiation pulse would be greater than 15 ns.

The gradient B experiments on SPEED at SNLA which reduced the risetime from 25 ns to 3 ns and the risetime sharpening predictions for Aurora (< 15 ns) developed in this report demonstrate that gradient B transport is a promising backup/alternative to the Merkeltron for reducing the risetime of the output radiation pulse on Aurora. Additional technical effort including resolution of the angle of incidence spectrum after transport and gradient B transport experiments on Aurora is clearly called for if the Merkeltron experiments do not provide the desired risetime sharpening.

SECTION 7

REFERENCES

1. C.R. Parsons, E.E. Holting, V.L. Kenyon, R.A. Smith, R.D. Genuario and V.L. Bailey, Proceedings of the 4th IEEE Pulsed Power Conference, Albuquerque, New Mexico, June 6-8, 1983, pg. 498.

2. James R. Lee, Robert C. Backstrom, John A. Halbleib, Jeffrey P. Quintenz, and Thomas P. Wright, J. Appl. Phys., 56, 3175 (1984).

3. V. Bailey, P. Champney, R. Genuario, I. Smith, and P. Spence, "Advanced Simulator Concepts Assessment Program", DNA-TR-81-233, Pulse Sciences, Inc., San Leandro, CA (1983).

4. J.R. Lee (private communication).

5. John A. Halbleib and Thomas W.L. Sanford, "Predicted Flash X-ray Evnironments Using Standard Converter Configurations", SNAD83-2572, Sandia National Laboratories, Albuquerque, NM (1983).

6. T.H. Martin, "Determination of Bremsstrahlung Production Efficiencies From Data Obtained on ⁻hermex at 27 MeV", SC-DR-69-240, Sandia National Laboratories, Albuquerque, NM (1982).

7. HWH/JCM, "Re-Evaluation of the Bremsstrahlung Production Efficiency For Optimum Targets", AWRE Internal Memo, August 1982.

8. Stewart E. Graybill, "AURORA Electron Beam Modification", HDL-TR-1862, Harry Diamond Laboratories, Adelphi, MD (1978).

9. P.F. Ottinger and Shyke A. Goldstein, Phys. Rev. Lett. 45, 340 (1980).

10. J.R. Lee, "Pulse Shaping of High-Current Electron Beams With Gradient B Drift Transport", SNAD86-0920, Sandia National Laboratories, Albuquerque, NM (1986).

DISTRIBUTION LIST

DNA-TR-88-98-V3

DEPARTMENT OF DEFENSE

ASSISTANT TO THE SECRETARY OF DEFENSE
ATOMIC ENERGY
ATTN EXECUTIVE ASSISTANT

DEFENSE INTELLIGENCE AGENCY
ATTN RTS-2B

DEFENSE NUCLEAR AGENCY
ATTN RAAE
ATTN RAEE
2 CYS ATTN RAEV
4 CYS ATTN TITL

DEFENSE NUCLEAR AGENCY
ATTN: TDNM
ATTN: TDTT
2 CYS ATTN: TDTT W SUMMA

DEFENSE TECHNICAL INFORMATION CENTER
2 CYS ATTN: DTIC/FDAB

OFFICE OF THE JOINT CHIEFS OF STAFF
ATTN: J BUTTS

DEPARTMENT OF THE ARMY

HARRY DIAMOND LABORATORIES
ATTN: SLCHD-NW-RA
ATTN: SLCHD-NW-RI KERVIS
ATTN: SLCIS-IM-TL (TECH LIB)

U S ARMY MISSILE COMMAND/AMSMI-RD-CS-R
ATTN: AMSMI-RD-CS-R (DOCS)

U S ARMY NUCLEAR & CHEMICAL AGENCY
ATTN: MONA-NU

U S ARMY TEST AND EVALUATION COMD
ATTN: AMSTE

USA SURVIVABILITY MANAGMENT OFFICE
ATTN: SLCSM-SE J BRAND

DEPARTMENT OF THE NAVY

NAVAL RESEARCH LABORATORY
ATTN: CODE 2000 J BROWN
ATTN: CODE 4700 S OSSAKOW
ATTN: CODE 4701 I VITOKOVITSKY
ATTN: CODE 4720 J DAVIS
ATTN: CODE 4770 G COOPERSTEIN

NAVAL SURFACE WARFARE CENTER
ATTN: CODE R4C

NAVAL SURFACE WARFARE CENTER
ATTN: CODE H-21

NAVAL WEAPONS CENTER
ATTN: CODE 343 (TECH SVCS)

DEPARTMENT OF THE AIR FORCE

ASSISTANT CHIEF OF STAFF
ATTN: AFCSA/SASA/W BARATTINO

SECRETARY OF AF/AQQS
ATTN: AF/RDQI

SPACE DIVISION/CNCIV
ATTN: YNV

SPACE DIVISION/XR
ATTN: XR (PLANS)

SPACE DIVISION/YA
ATTN: YAR
ATTN: YAS

SPACE DIVISION/YE
ATTN: SD/CWNZ

SPACE DIVISION/YG
ATTN: CNDA

WEAPONS LABORATORY
ATTN: SUL

DEPARTMENT OF ENERGY

DEPARTMENT OF ENERGY
ATTN: OFC OF INERT FUSION
ATTN: OFC OF INERT FUSION C HILLAND
ATTN: OFC OF INERT FUSION R SHRIEVER

LAWRENCE LIVERMORE NATIONAL LAB
ATTN: L-13 D MEEKER
ATTN: L-153
ATTN: L-545 J NUCKOLLS

LOS ALAMOS NATIONAL LABORATORY
ATTN: B259 MS J BROWNELL

SANDIA NATIONAL LABORATORIES
ATTN: C DRUMM
ATTN: J E POWELL
ATTN: M J CLAUSER
ATTN: D J ALLEN
ATTN: TECH LIB 3141

OTHER GOVERNMENT

CENTRAL INTELLIGENCE AGENCY
ATTN: OSWR/NED
ATTN: OSWR, J PINA

DEPARTMENT OF DEFENSE CONTRACTORS

ADVANCED RESEARCH & APPLICATIONS CORP
ATTN: R ARMISTEAD

AEROSPACE CORP
ATTN: LIBRARY ACQUISITION

BDM INTERNATIONAL INC
ATTN: E DORCHAK

BDM INTERNATIONAL INC
ATTN L O HOEFT

E SYSTEMS INC
ATTN C UBER

EOS TECHNOLOGIES, INC
ATTN B GABBARD

GENERAL ELECTRIC CO
ATTN H ODONNELL

IRT CORP
ATTN J M WILKENFELD
ATTN R MERTZ

JAYCOR
ATTN E WENAAS

JAYCOR
ATTN E WENAAS
ATTN R SULLIVAN

JAYCOR
ATTN C ROGERS

KAMAN SCIENCES CORP
ATTN D CALDWELL
ATTN S FACE

KAMAN SCIENCES CORP
ATTN E CONRAD

KAMAN SCIENCES CORPORATION
ATTN TECH LIB FOR/D PIRIO

KAMAN SCIENCES CORPORATION
ATTN DASIAC

KAMAN SCIENCES CORPORATION
ATTN DASIAC

LOCKHEED MISSILES & SPACE CO, INC
ATTN L CHASE

LOCKHEED MISSILES & SPACE CO, INC
ATTN S TAIMUTY

MAXWELL LABS, INC
ATTN A KOLB
ATTN M MONTGOMERY

MCDONNELL DOUGLAS CORPORATION
ATTN S SCHNEIDER

MISSION RESEARCH CORP
ATTN C LONGMIRE

MISSION RESEARCH CORP, SAN DIEGO
ATTN: V VAN LINT

PACIFIC-SIERRA RESEARCH CORP
ATTN: H BRODE, CHAIRMAN SAGE
ATTN L SCHLESSINGER

PHYSICS INTERNATIONAL CO
ATTN: C GILMAN
ATTN: C STALLINGS
ATTN: G FRAZIER

PULSE SCIENCES, INC
ATTN: I D SMITH
ATTN: P W SPENCE
ATTN: S PUTNOM
2 CYS ATTN: V BAILEY

R & D ASSOCIATES
ATTN: C KNOWLES
ATTN: P TURCHI

RAND CORP
ATTN: B BENNETT

S-CUBED
ATTN: A WILSON

SCIENCE APPLICATIONS INTL CORP
ATTN: K SITES

SCIENCE APPLICATIONS INTL CORP
ATTN: W CHADSEY

TRW INC
ATTN: D CLEMENT
ATTN: TECH INFO CTR, DOC ACQ

TRW SPACE & DEFENSE SYSTEMS
ATTN: D M LAYTON

FOREIGN

FOA 2
ATTN: B SJOHOLM

FOA 3
ATTN: T KARLSSON